



UNIVERSITY
OF WOLLONGONG
AUSTRALIA

University of Wollongong
Research Online

Faculty of Engineering and Information Sciences -
Papers: Part B

Faculty of Engineering and Information Sciences

2019

On Tetragonality of the Martensite Crystal Lattice in Steels

V Lobodyuk

National Academy of Sciences of Ukraine

Yu Ya Meshkov

National Academy of Sciences, Ukraine

Elena V. Pereloma

University of Wollongong, elenap@uow.edu.au

Publication Details

Lobodyuk, V. A., Meshkov, Y. Ya. & Pereloma, E. V. (2019). On Tetragonality of the Martensite Crystal Lattice in Steels. *Metallurgical and Materials Transactions A: Physical Metallurgy and Materials Science*, 50 (1), 97-103.

Research Online is the open access institutional repository for the University of Wollongong. For further information contact the UOW Library:
research-pubs@uow.edu.au

On Tetragonality of the Martensite Crystal Lattice in Steels

Abstract

This article addresses the pseudo-tetragonal nature of the crystal lattice of martensite in carbon-containing steels. It is proposed that the periodic distortion of c-cube edges by the presence of carbon atoms is better reflected in the root-mean-square distortions of martensite lattice than by the value of doublet splitting of the corresponding X-ray reflections of the martensite crystal.

Disciplines

Engineering | Science and Technology Studies

Publication Details

Lobodyuk, V. A., Meshkov, Y. Ya. & Pereloma, E. V. (2019). On Tetragonality of the Martensite Crystal Lattice in Steels. *Metallurgical and Materials Transactions A: Physical Metallurgy and Materials Science*, 50 (1), 97-103.

1 **On tetragonality of the martensite crystal lattice in steels**

2 V.A. Lobodyuk¹, Yu.Ya. Meshkov¹, E.V. Pereloma^{2,3*}

3 ¹ G.V. Kurdyumov Institute for Metal Physics, National Academy of Sciences of Ukraine, 36 Vernadsky Blvd., 03142,
4 Kiev, Ukraine

5 ² School of Mechanical, Materials, Mechatronic and Biomedical Engineering, University of Wollongong, New South
6 Wales 2522, Australia

7 ³ Electron Microscopy Centre, University of Wollongong, New South Wales 2500, Australia

8
9
10
11 **Abstract**

12 The paper addresses the pseudo-tetragonal nature of the crystal lattice of martensite in carbon-containing steels. It
13 is proposed that the periodic distortion of *c* cube edges by the presence of carbon atoms is better reflected in the
14 root mean square distortions of martensite lattice, than by the value of doublet splitting of the corresponding X-ray
15 reflections of the martensite crystal.

16
17
18 **Keywords:** martensite, carbon-containing steels, lattice structure, tetragonality

19
20
21
22 *Corresponding author: Ph. +612 4221 5507, email elenap@uow.edu.au

33 1. Introduction

34 Based on nearly hundred years of research, it is well known that martensite is formed in steels on quenching, due to
35 the diffusionless $\gamma \rightarrow \alpha'$ phase transformation. Since the late 1920s, when it was independently reported by Fink and
36 Campbell [1] and Seljakow et al. [2] that the lattice structure of quenched carbon steels is body centered tetragonal
37 (bct), the relationship between the carbon content and the lattice parameters received continued attention both in
38 experimental and modeling research. The original evidence for martensite (α' phase) lattice tetragonality came from
39 the splitting of (002) and (200) peaks [1,2] on X-ray diffractograms. It was established that a lattice parameter of
40 martensite (0.285 nm with accuracy of 0.0003nm) is always smaller than a lattice parameter (0.286 nm) of ferrite (α -
41 phase, body centered cubic, bcc). On the other hand, with an increase in carbon (C) content in the steel from 0.8 to
42 1.2 wt. %, the c lattice parameter of martensite increased from 0.291nm to 0.302 nm, corresponding c/a ratio
43 changes from 1.024 to 1.058. Due to an inability to resolve the diffraction doublets of the tetragonal lattice in steels
44 having C content < 0.6 wt. %, it was assumed that the c/a ratio in low carbon steels was 1. It was concluded [2] that
45 the coordinates of C atom were $00\frac{1}{2}$ in bct lattice, i.e. located along the tetragonal axis (c -axis). The observed
46 tetragonality of martensite lattice was explained by a statistical theory of the ordering of carbon in one preferred
47 sub-lattice, out of the three possible sub-lattices of octahedral interstices [3,4]. Such ordering is the result of the
48 Bain strain, which changes during homogeneous shear transformation the austenite lattice to martensite one and
49 positions carbon atoms located in the octahedral interstices of austenite lattice only in one out of three sub-lattices
50 of a new lattice [5], e.g. all C atoms are located on c -axis. Another explanation was given by Önman [6] proposing
51 that two C atoms with the axes of C_2 group parallel to the tetragonal axis of the lattice replace some of the iron
52 atoms. Zener [3] suggested that ordering of C atoms exists above (or below) a critical C concentration (or
53 temperature) at a definite temperature (or concentration). The resulting reduction in elastic energy due to ordering
54 dominates the decrease in entropy, thus leading to a decrease, instead of an increase, in free energy. However,
55 while the C atoms are ordered immediately on completion of austenite to martensite transformation, above the
56 critical temperature for a specific C concentration, C atoms having a sufficient mobility tend to randomize converting
57 the bct lattice to bcc. Based on Zeners' findings, the cubic-to-tetragonal transition at room temperature takes place
58 at approximately 0.6 wt. % C content in iron. Kurdjumov and Khachaturyan [4,7] also arrived at a similar conclusion
59 using a self-consistent theory of the order-disorder transition with static concentration waves and microscopic
60 elasticity theory. Revision of their calculations of the elastic interaction energy resulted in the critical C concentration
61 at room temperature being 0.18 wt.% [8,9]. Later on, this value for the cubic-to-tetragonal transition of first-order
62 nature was confirmed by Fan et al. [10] using a long-wavelength approximation for the stress-induced elastic
63 interaction in the theory of microscopic elasticity theory formulated by Khachaturyan [11].

64 Recently, using Rietveld refinement to deconvolute overlapping martensite peaks in data obtained from a high
65 resolution X-ray diffractometer, it was shown that martensite lattice is bct for a steel with 0.124 wt. %C
66 [12]. Tetragonality of martensite lattice due to C atoms ordering is manifested in appearance of martensite peaks
67 splitting on X-ray diffraction (XRD) patterns. Experimental evidence of disorder-order transitions was obtained by
68 Kritzkaya et al. [13,14] via subjecting a carbon steel (1 wt. % C) to neutron and electron radiation, which led to the
69 disappearance of martensite peak splitting in XRD patterns with the martensite lattice being indexed as bcc.
70 Subsequent prolonged holding at room temperature resulted in the reappearance of martensite doublet peaks
71 corresponding to a bct lattice. Such disordering \leftrightarrow ordering transition was observed to take place repeatedly during
72 several tests in the temperature interval from 293 K (20°C) to 228K (-45°C). Furthermore, the martensite lines
73 appear much less sharp compared to the austenite lines on XRD patterns. This was explained by Selyakov et al. [2] by
74 (i) formation of small martensite crystallites; (ii) inhomogeneity in carbon distribution and (iii) tetragonality of the
75 martensite lattice. However, even after prolonged homogenization treatment of Fe - (0.19-0.57) C - (5.50-9.18) Mn
76 - (1.62-5.5) Ni (wt. %) alloy for 36 h at 1473.15 K (1200°C), the martensite lines remained diffuse [15]. In order to
77 eliminate the effect of residual strain arising during martensite transformation in bulk, X-ray diffraction was carried
78 out on Fe powder with (0.8-1.5) wt. % C, but still showed diffuse martensite lines [16]. Thus, it could be suggested
79 that the diffusiveness of martensite lines on XRD patterns is also related to the martensite lattice tetragonality.

80 Furthermore, it could be supposed that this diffusiveness is related to the variations in the a and c lattice
81 parameters in neighboring unit cells, e.g. a set of a and c parameters exists in the crystal structure of martensite.

82 The XRD collects data from cube planes of different length, which manifests in the diffuse appearance of martensite
83 lines. It is well known that due to the diffusionless austenite to martensite transformation, only one C atom is
84 located in an octahedral interstice along the cube edge (c -axis) in the martensite lattice. However, C atoms are
85 absent on the other three cube edges, which are parallel to the c -axis. Thus, these three cube edges change their
86 length to a lesser extent; the degree of change depends on the distance of a particular cube edge to the one
87 distorted by the presence of C atom. Thus, such deformed crystal lattice could not be described as tetragonal, but
88 rather as *pseudo-tetragonal*. The diffuse appearance of martensite lines is also supported by the studies of static
89 lattice distortions resulting from martensite transformation in carbon steels [16,17]. The root mean square (RMS)
90 displacement of Fe atoms along c -axis $(\bar{u}_{st}^2)^{1/2}$ is twice as large compared to the two other axes, i.e. 0.0052 nm
91 versus 0.0025 nm, respectively [17]. The displacement depends on the separation between Fe and C atoms, which is
92 the smallest along c -axis. Such a lattice is not thermodynamically stable; it is metastable. The pseudo-tetragonality
93 observed by XRD is caused by strong elastic strains arising from the presence of interstitial C atoms in Fe lattice.

94 However, until now, it is accepted in both experimental and modelling works that the martensite lattice in carbon
95 steels is bct [12,19-24]. Thus, the aim of this paper is to clarify the nature of martensite lattice, as C concentrations
96 of 0.2-1.5 wt.% in steels are insufficient to form a proper bct lattice, and find out how the local distortions in crystal
97 structure result in a regular change of c lattice parameter manifested as pseudo-tetragonality.

98 99 2. Lattice distortions in bcc Fe due to the presence of interstitial C atoms

100 2.1. Dependence of martensite lattice parameters on C concentration in carbon steels

101 The original equation for a linear relationship between the lattice tetragonality and C content was formulated
102 according to Eq. 1 [22,23]:

$$103 \quad c/a = 1 + 0.045 \text{ wt. \% C} \quad (1)$$

104 Another empirical relationship was proposed [15]:

$$105 \quad c/a = 1 + 0.0467 \text{ wt. \% C} \quad (2)$$

106 On another hand, Cheng et al. [24] using 0.28664 nm as the lattice parameter of pure bcc-iron at 300 K (26.85°C)
107 established the linear dependences of lattice tetragonality ratio (Eq.3) for the bct iron-carbon martensite a and c
108 parameters; the latter were determined as functions of the number of interstitials per 100 iron atoms, X_c :

$$109 \quad c/a = 1 + (0.95 \pm 0.01) X_c \quad (3)$$

110 This relationship was further modified to Eq. 4 [12]:

$$111 \quad c/a = 1 + 0.031 \text{ wt. \% C} \quad (4)$$

112 A summary of the literature data on the variation of c/a ratio as a function of carbon content is given in Fig. 1. It is
113 seen, that all experimental data fits reasonably well to linear relationships. Some deviations, as well as differences
114 between the linear relationships, are related to the accuracy of measurements of lattice peaks positions and
115 concentration of C atoms. It is seen that earlier data was available only for martensite of ≥ 0.6 wt.% C [6,15,22] due
116 to the techniques limitations, whereas more recent one also covers 0.128-0.6 wt. % C range [12, 25]. It should be
117 also noted that data from Ref. [25] is the theoretical one.

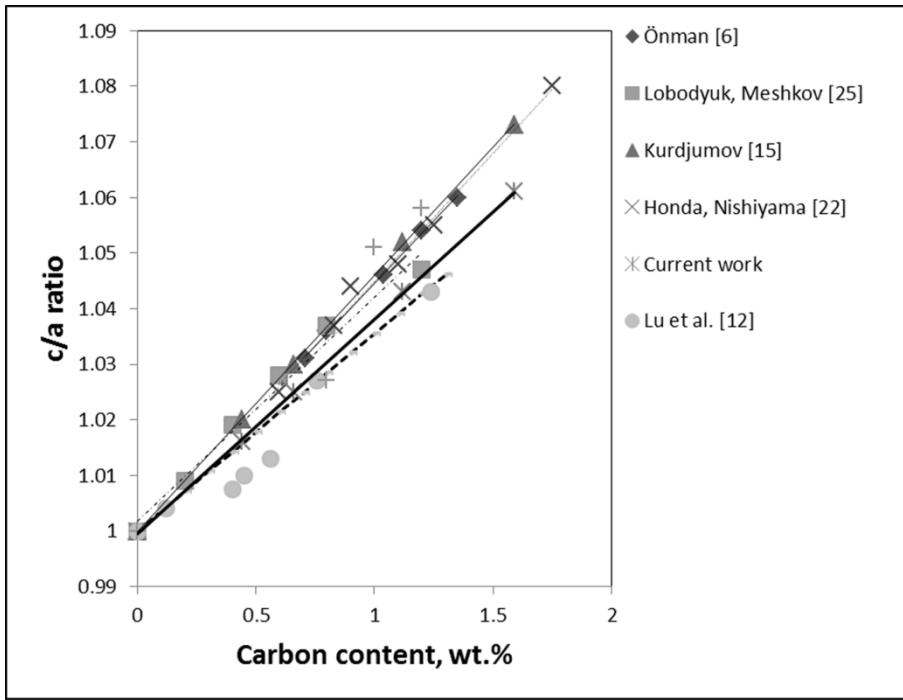


Fig. 1 Effect of carbon content in martensite on c/a ratio.

2.2. Distortion of bcc lattice in Fe due to interstitial C atoms

The high temperature phase of austenite contains C atoms in octahedral interstices located in the centre of face-centered cubic lattice. The lattice distortion of austenite is minimal in this case and a_γ lattice parameter increases as a function of C content in austenite according to Eq. 5 and Table 1 [25]:

$$\alpha_\gamma = 0.35586 + qp \quad (5)$$

where 0.35586 nm is austenite lattice parameter of pure Fe; p is the C content in austenite, wt. %, and q is a distortion of austenite lattice parameter due to addition of 1 wt. % C (Table 1): $q = (0.0032 \pm 0.0001)$ nm.

In two neighboring fcc lattices of austenite one body-centered tetragonal unit cell, bct, could also be identified as shown in Fig. 2a.

Thus, the lattice parameters of austenite could be expressed for both types of lattices as:

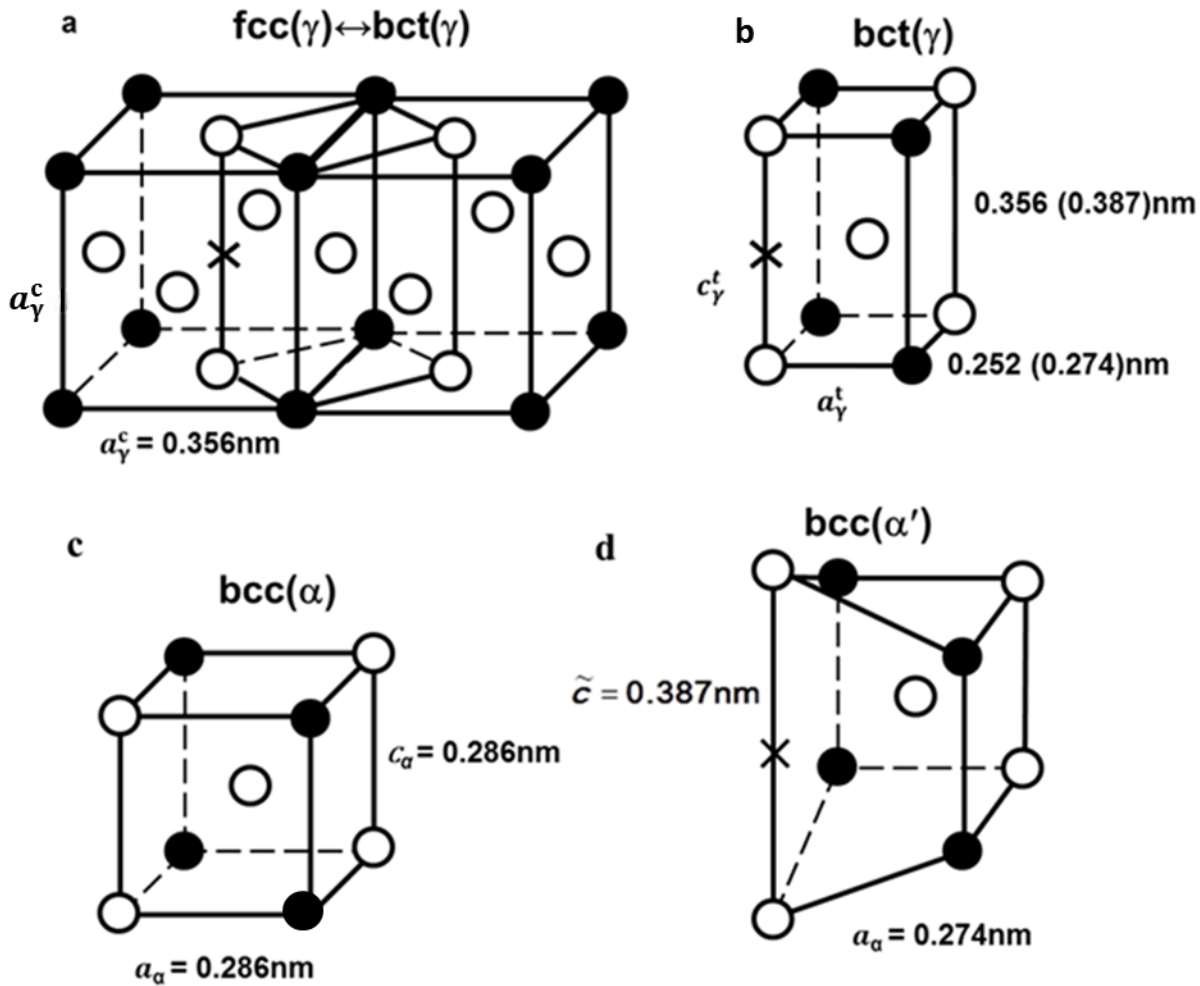
in fcc:

$$a_\gamma^c = b_\gamma^c = c_\gamma^c \quad (6)$$

and in bct:

$$c_\gamma^t = \sqrt{2} a_\gamma^t = \sqrt{2} b_\gamma^t \quad (7)$$

For pure Fe: $a_\gamma^c = b_\gamma^c = c_\gamma^c = 0.35586$ nm, whereas from Eq. 7 follows $a_\gamma^t = c_\gamma^t / \sqrt{2} = 0.2524$ nm.



140

141 Fig. 2. Schematic representation of Fe crystal lattices:

142 a – The bct lattice of γ -Fe in two unit cells of fcc; ● – position of corner Fe atoms in fcc lattice; o – position of Fe
 143 atoms on the faces of fcc lattice; x – possible positions of C atoms.

144 b – The bct lattice of γ -Fe. Parameters are given for carbon-free Fe and in brackets for carbon-containing ones.

145 c – The bcc lattice of pure Fe after $\gamma \rightarrow \alpha$ – transformation.

146 d – Distorted bcc Fe $_{\alpha}$ lattice, having C atom cube edge, \tilde{c} (x – indicates the position of C atom).

147

148 For austenite with full occupancy of octahedral interstices by carbon ($n_{at} = 33$ at. %, $p = 9.7$ wt. %), these values
 149 according to Eq. 5 are: $a_{\gamma}^c = b_{\gamma}^c = c_{\gamma}^c = 0.3869$ nm; $c_{\gamma}^t = c_{\gamma}^c = 0.3869$ nm and $a_{\gamma}^t = c_{\gamma}^t / \sqrt{2} = 0.2744$ nm (see
 150 Fig. 2b).

151 When C atoms are located at the middle of cube edge of bct austenite lattice, the distance between the
 152 corresponding two Fe atoms increases, e.g. cube edge c_{γ}^t . In order to estimate this increase, the value of c_{γ} could be
 153 extrapolated using Eq. 5 for a such hypothetical C concentration in which one C atom is located at each one of four
 154 cube edges [25,26]. Calculations showed that in this case there are two Fe atoms and one C atom per bct unit cell;
 155 three atoms in total. The atomic concentration of carbon in such austenite is 1/3, which correlates to weight
 156 concentration $p = 9.7$ wt. % determined using the following Eq. 8:

$$p(\%) = \frac{12n_{at}}{12n_{at} + 56(1-n_{at})} \quad (8)$$

157

158 where n_{at} is atomic concentration of carbon in steel, at. %.

159 At the same time, according to Eq. 5, $c_{\gamma}^t = 0.38686$ nm, e.g. the distance between two Fe atoms and C atom, inserted
160 between them, should be ~ 0.387 nm (Fig. 2d). During the $\gamma \rightarrow \alpha'$ transformation for a bct lattice to revert to a bcc
161 lattice (Fig. 2c), the c axis is compressed and a and b axes are expanded uniformly as the result of Bain strain.

162 If one were to assume that following $\gamma \rightarrow \alpha'$ transformation during quenching the C atom remained in the same
163 position relative to the Fe atoms, albeit in the distorted bct lattice of martensite (Fig.2d), then the c axis length
164 would remain the same ($c = 0.387$ nm). However, this cube edge containing C atom is extended compared to other
165 three cube edges (in c-axis direction) which are free from carbon atom according to Eq. 9:

$$166 \frac{\tilde{c}}{a_{\alpha}} = \frac{0.387}{0.286} = 1.35 \quad (9)$$

167 Taking into account that the lattice parameter a_{α} in the martensite lattice decreases with increasing carbon
168 concentration in steel [15], for the case when $p = 9.7$ wt. % and $a_{\alpha} = 0.274$ nm the relative extension of edge cube \tilde{c}
169 (Eq. 9) would be ~ 1.41 , which correlates to $\sqrt{2}$. Thus, the assumed maximum degree of tetragonality of the
170 martensite lattice when carbon atoms are present on all cube edges parallel to c-axis is $\sqrt{2}$. However, as only one
171 cube edge is occupied by a C atom, the experimentally determined martensite lattice tetragonality is well below $\sqrt{2}$.
172 It also depends on the concentration of carbon, which determines the average number of cube edges containing C
173 atoms. This dependence on the carbon content in steel can be modelled.

174

175 3. Model for calculation of the average value for the c parameter of martensite lattice.

176 Calculations were undertaken for a limited volume of martensite crystal having a square cross-section and one α'
177 phase lattice parameter thickness. This volume has the shape of compressed prism, for which the total number of Fe
178 and C atoms always equals to 100 and where the Fe/C ratio changes according to the atomic concentration of
179 carbon in the steel. Consequently, the number of unit lattices (and the number of cube edges c) decreases with an
180 increase in the number of C atoms, as the number of Fe atoms forming the unit cell decreases. 100 Fe atoms form 50
181 unit lattices with one individual c cube edge each. However, in the Fe-33 at.% C alloy, there are 67 Fe atoms, which
182 form only 33 unit lattices containing 33 cube edges of increased size $\tilde{c} = \sqrt{2} a$; the tetragonality of the lattice in such
183 alloy is the maximum possible: $c/a = \sqrt{2} a$. In all alloys having an intermediate carbon content, the number m of
184 increased cube edges \tilde{c} will vary from 0 to 33 depending on carbon concentration (Table 2):

$$185 m = 100 [1 - 0.5 (1 - n_{at})] \quad (10)$$

186 where n_{at} is concentration C in at. %.

187 Depending on the carbon concentration in the martensite, the ratio of the fraction p of increased cube edges \tilde{c} to
188 the fraction s of regular cube edges with $c = a$, changes (Table 2). In the current model, the crystal of martensite is
189 presented as a set of unit lattices of practically regular bcc lattice with lattice parameters $a = b \approx c$, among which a
190 certain number of sets of four significantly distorted bcc lattices exists, which are combined in a single block with a
191 common extended cube edge $c = \sqrt{2} a$ (Fig. 3b c.f. with 4 unit cells of ferrite shown in Fig. 3a).

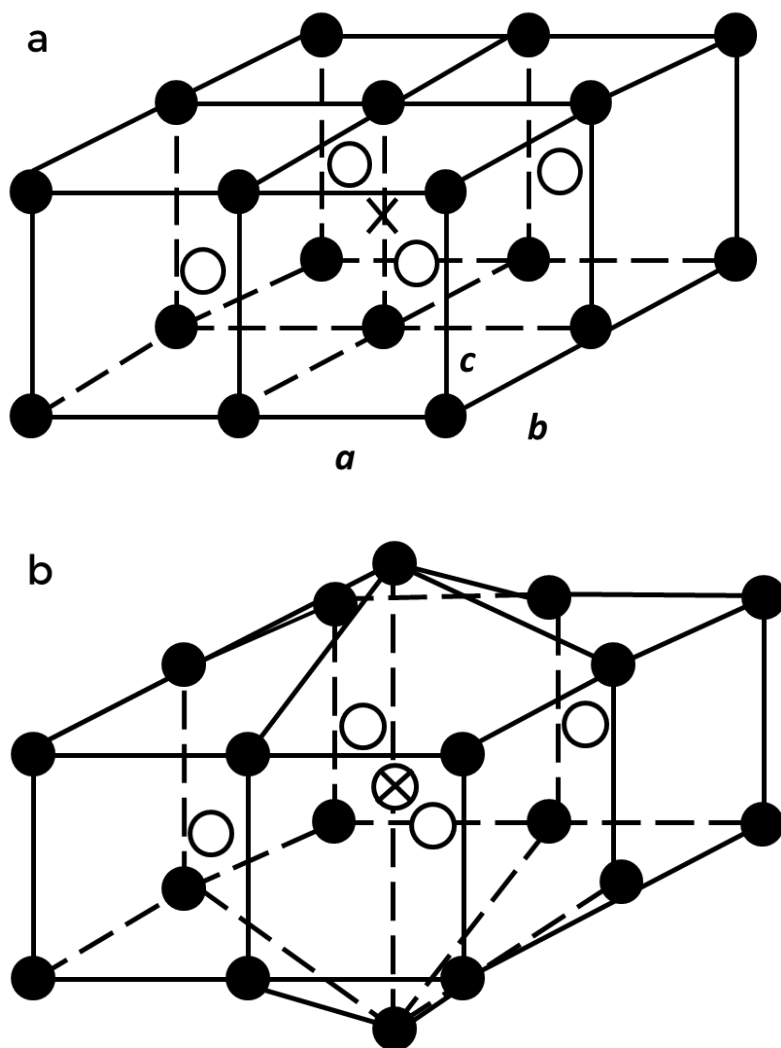
192 Such a theoretical block of 4 bcc unit cells of Fe is the minimum volume of martensite crystal, in which the averaged
193 tetragonality of the lattice could be expressed if were distributed uniformly among all four cube edges the
194 anomalous extension of one common cube edge with $\tilde{c} = 1.41a$:

$$195 \frac{\bar{c}}{a} = \frac{1.4a + 3a}{4} = 1.1 \quad (11)$$

197 Despite using such a rough approximation and ignoring any possible effects of anomalous cube edge exhibiting a \tilde{c}
 198 length extension of other cube edges of the same block structure, as could be seen below, this approach is a
 199 reasonable one for explaining the physical basis for the pseudo-tetragonality of martensite lattice in quenched
 200 carbon steels observed using XRD. If one were to imagine the condition where the entire martensite crystal is
 201 formed only by blocks comprising such four unit cells, then the observed by XRD tetragonality should be $\bar{c}/a = 1.10$.
 202 This condition (1 C atom + 8 Fe atoms) corresponds to the Fe-C alloy containing 11 at. % C (2.5 wt. % C). Thus,
 203 according to Eq. 2, c/a ratio is 1.12. It could be assumed that $c/a \approx 1.1$ (Eq. 11) is the maximum possible value which
 204 could be obtained experimentally for martensite pseudo-tetragonality for quenched-in martensite of this
 205 composition.

206

207



208

209

210

211 Fig. 3. Model of the block consisting of 4 lattice unit cells of:

212 a – α -phase, bcc, ferrite.

213 b – block containing one common extended cube edge \tilde{c} due to the presence of C atom at the middle (average
 214 pseudo-tetragonality is $\bar{c}/a \approx 1.1$). x – indicates the position of C atom. • – position of corner Fe atoms in fcc lattice;
 215 o – position of Fe atoms on the faces of fcc lattice; x – possible positions of C atoms.

217 Similarly, the averaging of all cube edges c for the lattice containing 100 (Fe + C) atoms could be performed for all
 218 different atomic concentrations of carbon (Table 2) and the corresponding averaged length of cube edge \bar{c} could be
 219 calculated. These calculations resulted in the following relationship for averaged lattice pseudo-tetragonality and the
 220 atomic carbon concentration (Eq.12) and presented as data for this work in Fig. 1:

$$221 \quad \frac{\bar{c}}{a} = 1 + 0.41p \quad (12)$$

222 These calculations differ from the experimentally observed relationships (linear for Ref. [15], Fig. 1) by angle
 223 coefficient $\gamma = 0.0467$ from Eq. 2 [15], a difference of only 12 %. These lower theoretical values compared to XRD
 224 data could be due to not taking into account the effect of the extended cube edge \tilde{c} on the length of neighboring C-
 225 free cube edges. The proposed model for explanation of averaged tetragonality of martensite lattice is reasonable as
 226 the error for determination of parameter \bar{c} is ± 0.002 nm and for determination of c/a ratio it is less than 0.6 % (for
 227 Fe-1wt. % C alloy). It should be also noted that calculated data using this model (Fig. 1) is located between the old
 228 data determined in the 1930-70s and the more recent, refined results of Lu et al. [12].

229

230 4. Discussion

231 Proposed model is only a rough approximation, as further refinement and a better correlation with experimental
 232 data could be achieved by incorporation of the precise length of C-free cube edges neighboring the extended $\tilde{c} = \sqrt{2}$
 233 a one.

234 The main outcome of the proposed model lies not in the good fit with experimental data, but in the suggestion that
 235 the crystal α' -lattice of quenched steel does not exhibit tetragonality by nature, but presents a system of regular bcc
 236 unit lattices of α -Fe with inclusions of special blocks of four distorted bcc unit lattices (Fig. 2b), the main
 237 characteristics of which is the presence in the middle of the block of one extended cube edge with $\tilde{c} = \sqrt{2} a$ length.
 238 The latter is responsible for the specific biconvex 'tent-shape' of the block (Fig. 3b). The average value of cube edges
 239 c in such 'tent' is approximately $\bar{c}/a \approx 1.1a$, which could be considered as a manifestation of the pseudo-
 240 tetragonality of α' -lattice block with $c/a \approx 1.1$.

241 Depending on the C content, the density of blocks increases leading to the observation of doublets of {101}, {002}
 242 (and others). For the last 80 years this has been explained as the averaged tetragonality of martensite α' -lattice
 243 dependent on C content, but which physically, in reality, does not exist. The averaged parameter \bar{c} manifests in the
 244 appearance of diffraction doublets, whereas the variations from $c=a$ to $c=\bar{c}$ are reflected in the degree of widening of
 245 corresponding diffraction lines.

246 The physical reason for the experimentally observed pseudo-tetragonality of martensite lattice is ordering of carbon
 247 atoms in the Fe-lattice at the midpoint of selected cube edges. This leads to the extension of these cube edges (\tilde{c})
 248 compared to the regular carbon-free ones ($c_\alpha = a_\alpha$). Reduction in the degree of C atom ordering along cube edges c_α
 249 and C content in steel leads to the decrease in the lattice pseudo-tetragonality ratio c/a and finally to formation of
 250 bcc martensite.

251 The crystal structure of the martensite lattice containing interstitial C atoms in the lattice should therefore be
 252 described as pseudo-tetragonal one. Appearance of this pseudo-tetragonality phenomenon is due to the statistical
 253 averaging of displacement of Fe atoms in α' -lattice. Static lattice distortion measurement using XRD suggests that
 254 the RMS displacements of atoms from their lattice positions ($\langle \bar{u}_{st}^2 \rangle^{1/2}$) are related to the variations in the length of
 255 cube edges c in α' -phase. For example, according to Ref. [18], the value for this RMS distortion of α' -phase lattice for
 256 martensite with 1wt. % C is 0.01nm. In this case, the interstitial C atom displaces Fe atoms on both sides of cube
 257 edge and therefore the RMS extension of the c is 0.02 nm. The average length of the extended cube edge is:

258 $\bar{c} = 0.286 + 0.02 = 0.306 \text{ nm}$ (13)

259 From Eq. 13 follows:

260 $\frac{\bar{c}}{a} = \frac{0.306}{0.286} = 1.07$ (14)

261 The experimental value of c/a (Eq. 2) for the same Fe-C alloy is 1.05. There is little advantage in trying to improve
262 the prediction of the \bar{c}/a value based on the RMS lattice distortions of α' -phase in quenched steel, as the high
263 density of dislocations [4] in martensite also contributes to this term. This explains a higher \bar{c}/a value obtained in
264 Ref. [13].

265 5. Conclusions

- 266 1. It is reasonable to consider crystal structure of the martensite in carbon-containing steels as pseudo-tetragonal.
- 267 2. It is suggested that origin of the pseudo-tetragonality is result of the periodic distortion of c cube edges. This
268 distortion is best represented by the RMS of the static distortions of the martensite lattice ($\langle \bar{u}_{st}^2 \rangle^{1/2}$) rather than by
269 the value of doublet splitting of the corresponding X-ray reflections of the martensite crystal.
- 270 3. The small difference between the values obtained using both approaches is not important, as in both cases the
271 assumed value of pseudo-tetragonality c/a does not reflect the real crystalline nature of martensite lattice and is
272 simply an accepted term for lattice description.
- 273 4. The atomic-crystalline structure of martensite of carbon steel is best referred to as pseudo-tetragonal one (or
274 "tetragonal-like") and distortions of the α' -lattice describe the average distortions, rather than represent a true
275 tetragonality.

276

277 References

- 278 1. W. L. Fink and E. D. Campbell, Trans. Am. Soc. Steel Treat. 1926, vol. 9, pp.717-52.
- 279 2. N. Seljakow, J. Kurdumoff and N. Goodtzov, Nature, 1927, vol.119, p. 494.
- 280 3. C. Zener, Trans. AIME, 1946, vol. 167, pp. 550–95.
- 281 4. A. G. Khachaturyan, Theory of Phase Transformations and Structure of Solid Solutions, Nauka, Moscow,
282 1974, 384 p. [in Russian].
- 283 5. E. Bain, Trans. AIME, 1924, vol. 70, 25-46.
- 284 6. E. Önman, Nature, 1931, vol. 127 (No.3199), pp. 270-72.
- 285 7. G. V. Kurdjumov and A. G. Khachaturyan, Metall. Trans., 1972, vol. 3, pp.1069-76.
- 286 8. G. V. Kurdjumov and A. G. Khachaturyan, Acta Metall., 1975, vol. 23, 1077-1088.
- 287 9. G. V. Kurdjumov, Metall. Trans. 1976, vol. 7A, pp. 999-
- 288 10. Z. Fan, L. Xiao, Z. Jinxiu, K. Mokuang and G. Zhenqi, Phys. Rev. B, 1995, vol. 52 (14), pp. 9979-87.
- 289 11. A.G. Khachaturyan, Sov. Phys. Solid State 1963, vol.5, pp.750-758 [in Russian].
- 290 12. Y. Lu, H. Yu, R.D. Sisson Jr., Mater Sci Eng. A, 2017, vol. 700, pp. 592-597.
- 291 13. V.K. Kritzkaya, V.A. Il'ina, DAN USSR, 1969, vol. 185, pp.1273 -1275 [in Russian].

- 292 14. V.K. Kritzkaya. In: Defects of crystallographic structures and Martensitic Transformations. Nauka, Moscow,
293 USSR, 1972, pp. 94-100 [in Russian].
- 294 15. G.V. Kurdjumov, Phenomena of quenching and tempering in steel. Metallurgizdat, Moscow, USSR, 1961, 64
295 p. [in Russian].
- 296 16. M.P. Arbuzov, DAN USSR, 1950, vol. 74, pp.1085-88 [in Russian].
- 297 17. M.P. Arbuzov, L.I. Lysak, E.G. Nesterenko, DAN USSR, 1953, vol. 90, pp. 375-77 [in Russian].
- 298 18. B. G. Lifshitz, Physical Properties of Metals and Alloys. Mashgiz, Moscow, USSR, 1959, 368 p. [in Russian].
- 299 19. H. Ohtsuka... ISIJ Int., 2015, vol. 55, pp.2483-91.
- 300 20. D.A. Mirzaev, A.A. Mirzoev, P.V. Chirkov, 2016, vol. 843, pp. 195-200.
- 301 21. S. Chentouf, S. Cabutts, F. Danoix.... Intermetallics, 2017, vol. 89, pp.92-99.
- 302 22. K. Honda, Z. Nishiyama, Sci. Rpts. Tohoku. Imp. Univ. Ser. 1, 1932, vol. 21, p. 299.
- 303 23. M. Cohen, Trans. AIME, 1962, vol. 224, pp. 638-54.
- 304 24. L. Cheng, A. Böuger, Th.H. de Keijser, E.J. Mittemeijer, Scr. Mater. 1995, vol. 24, pp. 509-14.
- 305 25. V.A. Lobodyuk, Yu.Ya. Meshkov, Metallofiz. Nov. Techn., 2017, vol. 39, pp. 1281- 1298 [in Russian].
- 306 26. Yu.Ya. Meshkov, V.A. Lobodyuk, Metallofiz. Nov. Techn., 2017, vol. 39, pp.1423-1433 [in Russian].

307

308

309 Figure captions.

310 Fig. 1 Effect of carbon content in martensite on c/a ratio.

311 Fig. 2 Schematic representation of Fe crystal lattices:

312 a – The bct lattice of γ -Fe in two unit cells of fcc; ● – position of corner Fe atoms in fcc lattice; o – position of Fe
313 atoms on the faces of fcc lattice; x – possible positions of C atoms.

314 b – The bct lattice of γ -Fe. Parameters are given for carbon-free Fe and in brackets for carbon-containing ones.

315 c – The bcc lattice of pure Fe after $\gamma \rightarrow \alpha$ – transformation.

316 d – Distorted bcc Fe_α lattice, having C atom cube edge, \tilde{c} (x – indicates the position of C atom).

317 Fig. 3. Model of the block consisting of 4 lattice unit cells of:

318 a – α -phase, bcc, ferrite.

319 b – block containing one common extended cube edge \tilde{c} due to the presence of C atom at the middle (average
320 pseudo-tetragonality is $\tilde{c}/a \approx 1.1$). x – indicates the position of C atom.

321 ● – position of corner Fe atoms in fcc lattice; o – position of Fe atoms on the faces of fcc lattice; x – possible positions
322 of C atoms.

323

Phase	Carbon content, wt.%	Average number of atoms in the unit cell	Lattice parameters a and c , nm	Tetragonality, c/a
Ferrite, bcc	0	2.000	0.2861	1.00
Austenite, fcc	0	4.000	3.5586	1.00
	0.2	4.037	3.5650	
	0.4	4.089	3.5714	
	0.6	4.156	3.5778	
	0.8	4.224	3.5842	
	1.0	4.291	3.5906	
	1.4	4.427	3.6034	
Martensite	0	2.000	$a = 0.2861$	1.000
	0.2	2.018	$c = 0.2861$	1.009
	0.4	2.036	$a = 0.2858$	1.019
	0.6	2.056	$c = 0.2885$	1.028
	0.8	2.075	$a = 0.2855$	1.037
	1.2	2.094	$c = 0.2908$	1.047
	1.4	2.132	$a = 0.2852$	1.065
			$c = 0.2932$	
			$a = 0.2849$	
			$c = 0.2955$	
			$a = 0.2846$	
			$c = 0.2979$	
			$a = 0.2840$	
			$c = 0.3026$	

330 Table 2. Parameters for calculations of average value \bar{c}' for cube edge distorted by carbon atoms in martensite
 331 lattice as a function of carbon content (per 100 atoms of Fe-C alloy)

332

at.% C	wt.% C	Number of C atoms per 100 Fe-C atoms	Number of Fe atoms per 100 Fe-C atoms	Number of unit cells α -Fe	Total number of individual c-edges	Number of distorted edges \bar{c}	Number of regular, non- distorted c- edges, s	Mean relative length of c- edge, \bar{c}' $/a$	Tetragonal ity, Eq. 2 [15]
0	0	0	100	50	50	0	50	1.000	1.000
2	0.44	2	98	49	49	2	47	1.016	1.020
3	0.66	3	97	48	48	3	45	1.025	1.030
5	1.12	5	95	47	47	5	42	1.043	1.052
7	1.59	7	93	46	46	7	39	1.061	1.073
10	2.33	10	90	45	45	10	35	1.090	1.107
20	5.10	20	80	40	40	20	20	1.200	1.230
33	9.70	33	67	33	33	33	33	1.400	1.450

333